

Large-mass neutron stars with hyperonization

Wei-Zhou Jiang

*Department of Physics, Southeast University, Nanjing 211189, China
and Center of Theoretical Nuclear Physics, National Laboratory of Heavy Ion Accelerator, Lanzhou 730000,
China*

Bao-An Li

*Department of Physics and Astronomy, Texas A&M University-Commerce, Commerce, TX 75429, USA
and Department of Applied Physics, Xian Jiao Tong University, Xian 710049, China*
and

Lie-Wen Chen

*INPAC, Department of Physics and Shanghai Key Laboratory for Particle Physics and Cosmology,
Shanghai Jiao Tong University, Shanghai 200240, China
and Center of Theoretical Nuclear Physics, National Laboratory of Heavy Ion Accelerator, Lanzhou 730000,
China*

ABSTRACT

Within a density-dependent relativistic mean-field model using in-medium meson-hadron coupling constants and meson masses, we explore effects of in-medium hyperon interactions on properties of neutron stars. It is found that the hyperonic constituents in large-mass neutron stars can not be simply ruled out, while the recently measured mass of the millisecond pulsar J1614-2230 can constrain significantly the in-medium hyperon interactions. Moreover, effects of nuclear symmetry energy on hyperonization in neutron stars are also discussed.

Subject headings: dense matter - equation of state - stars: neutron

1. Introduction

The in-medium hyperon interactions play an important role in determining properties of hypernuclei and the hyperonization in neutron stars. Conversely, observed properties of hypernuclei and neutron stars can be used to constrain the in-medium hyperon interactions. For instance, it has been shown that the properties of hypernuclei are indeed very useful in extracting in-medium hyperon potentials at subsaturation densities (Friedman & Gal 2007). In bulk matter, such as neutron stars, hyperons can be produced by virtue of strong interactions. They can actually become important constituents of neutron stars and thus have important effects on astrophysi-

cal observations (for a review, see (Glendenning 2001)). In fact, it is well known that the hyperonization can reduce the maximum mass of neutron stars as much as $3/4M_{\odot}$ (Glendenning 1985; Glendenning & Moszkowski 1991; Jiang 2006). Currently, a number of phenomenological models, considering only the minimum compositions of nucleons and leptons using interaction parameters that are well calibrated by using terrestrial nuclear laboratory data, can produce the maximum mass of neutron stars around or below $2M_{\odot}$ (Danielewicz & Lacey 2002; Piekarewicz 2007). Interestingly, several neutron stars with large masses around $2M_{\odot}$ have been observed (Nice et al. 2005, 2008; Özel 2006) recently. In particular, the $2M_{\odot}$ pulsar J1614-

2230 was measured rather accurately through the Shapiro delay (Demorest et al. 2010). Since properties of neutron stars are determined by the nuclear equation of state (EOS) and the hyperonization reduces significantly the maximum mass of neutron stars, it has been stated that these observations seem to rule out almost all currently proposed hyperon EOS. Recent evidence for this can also be found in the work of the Brueckner approach (Schulze & Rijken 2011).

Though most of the hyperon EOSs give lighter neutron stars, there were actually a few endeavors in the past to stiffen the EOS either by invoking strong repulsions for hyperons or pushing upwards the onset density of hyperons, leading to heavy neutron stars involving hyperons (Hofmann et al. 2001; Takatsuka et al. 2002; Stone et al. 2007; Dexheimer & Schramm 2008). Recently, by virtue of nonlinear self-interacting terms involving a vector meson with hidden strangeness, Bednarek et al. obtained a stiff hyperon EOS with which the large mass of the PSR J1614-2230 can be produced (Bednarek et al. 2011). Usually, the SU(6) relations are imposed to constrain the meson-hyperon coupling constants. Such SU(6) relations were recently reexamined by Weissenborn et al. and an arbitrary breaking of such relations can also result in the stiffening of hyperon EOS and the uplift of the maximum mass of neutron stars with the inclusion of hyperons (Weissenborn et al. 2011a). On the other hand, the quark deconfinement may occur in the medium as the spatial overlap of nucleons becomes sufficient to dissolve the boundary of color singlets with the increase of density. Of course, the quantitative understanding of such a color deconfinement in cold medium is still model dependent. Typical effective QCD models include the NJL-like models, e.g., see (Klöhn et al. 2007; Ippolito et al. 2008; Pagliara & Schaffner 2008; Bonanno & Sedrakian 2011) and widely used MIT bag models, e.g., see (Prakash et al. 1997; Alford et al. 2005; Weissenborn et al. 2011b), as well as Schwinger-Dyson approaches (Li and Luo et al. 2011). With the Maxwell or Gibbs constructions for the hadron-quark phase coexistence, the resulting quark EOS may give rise to two possible types of stars: strange stars which are totally made of absolutely stable strange matter (Glendenning 2000) and hybrid stars with a quark core and

hadron out-layer. In order to be consistent with the recent observation of the $2M_{\odot}$ pulsar, the strong coupling and/or color superconductivity were shown to be necessary (Xu 2003; Alford et al. 2005; Klöhn et al. 2007; Ippolito et al. 2008; Pagliara & Schaffner 2008; Weissenborn et al. 2011b; Bonanno & Sedrakian 2011). While the compositions of hybrid stars are rather model dependent, it is interesting to mention that Yasutake et al. suggested the hyperon suppression with the MIT model using a density-dependent bag constant (Yasutake et al. 2011).

Noticing the recent investigations on the consequences of various quark EOS, we examine in this work the consistency of the hyperon EOS with the recent observation of the PSR J1614-2230. Despite the impressive progress made in recent decades in constraining the nuclear EOS using both astrophysical observations and nuclear reaction data, see, e.g. (Youngblood et al. 1999; Danielewicz & Lacey 2002; Li et al. 2008), many uncertainties still remain. The in-medium hyperon interactions are among the most uncertain ingredients of neutron star models. We shall thus seek in-medium hyperon interactions that can produce the observed maximum mass of neutron stars. In view of the fact that some microscopic theories, such as the Brueckner approach, are still having difficulties to obtain the $2M_{\odot}$ of hyperonized neutron stars, here we resort to the phenomenological models developed in refs. (Jiang et al. 2007a,b) to analyze effects of various in-medium hyperon interactions on properties of neutron stars.

2. Density-dependent relativistic mean-field models and parametrizations

In order to study conveniently the in-medium interactions for hyperons, we seek for density-dependent relativistic models without nonlinear interactions. In our previous works (Jiang et al. 2007a,b), we constructed density dependent relativistic mean-field (RMF) models using in-medium hadron properties according to the Brown-Rho scaling due to the chiral symmetry restoration at high densities (Brown & Rho 1991; Song 2001; Brown & Rho 2005; Brown et al. 2007). In these models, the symmetric part of the resulting equations of state around normal den-

sity is consistent with the data of nuclear giant monopole resonances (Youngblood et al. 1999) and at supra-normal densities it is constrained by the collective flow data from high energy heavy-ion reactions (Danielewicz & Lacey 2002), while the resulting density dependence of the symmetry energy at sub-saturation densities agrees with that extracted from the isospin diffusion data from intermediate energy heavy-ion reactions (Tsang et al. 2004; Chen et al. 2005; Li & Chen 2005). Our models with the chiral limits are soft at intermediate densities but stiff at high densities naturally, producing a heavy maximum neutron star mass around $2M_\odot$. It is interesting to see that the EOS extracted from the celestial observations most recently features similar characters (Steiner et al. 2010). Apart from the usual studies on the minimum constituents in neutron stars with electrons, protons and neutrons, in this work we include the hyperonic degrees of freedom to study the in-medium interactions for hyperons with the constraints of the recent celestial observations. The model Lagrangian with the density-dependent parameters is written as

$$\begin{aligned} \mathcal{L} = & \bar{\psi}_B [i\gamma_\mu \partial^\mu - M_B^* + g_{\sigma B}^* \sigma - g_{\omega B}^* \gamma_\mu \omega^\mu \\ & - g_{\rho B}^* \gamma_\mu \tau_3 b_0^\mu] \psi_B + \frac{1}{2} (\partial_\mu \sigma \partial^\mu \sigma - m_\sigma^{*2} \sigma^2) \\ & - \frac{1}{4} F_{\mu\nu} F^{\mu\nu} + \frac{1}{2} m_\omega^{*2} \omega_\mu \omega^\mu - \frac{1}{4} B_{\mu\nu} B^{\mu\nu} \\ & + \frac{1}{2} m_\rho^{*2} b_{0\mu} b_0^\mu + \mathcal{L}_Y + \mathcal{L}_l, \end{aligned} \quad (1)$$

where ψ_B , σ , ω , and b_0 are the fields of the baryons, scalar, vector, and isovector-vector mesons, with their masses M_B^* , m_σ^* , m_ω^* , and m_ρ^* , respectively. $F_{\mu\nu}$ and $B_{\mu\nu}$ are the strength tensors of the ω and ρ mesons, respectively. The meson coupling constants and masses with asterisks denote the density dependence, given by the BR scaling (Jiang et al. 2007a,b). \mathcal{L}_l and \mathcal{L}_Y are the Lagrangian for leptons and hyperons, respectively. The parameters for strange mesons σ^* (i.e. f_0 , 975 MeV) and ϕ (1020 MeV) in \mathcal{L}_Y are assumed to be density independent.

The energy density and pressure in the RMF approximation read, respectively,

$$\begin{aligned} \mathcal{E} = & \frac{1}{2} m_\omega^{*2} \omega_0^2 + \frac{1}{2} m_\rho^{*2} b_0^2 + \frac{1}{2} m_\phi^2 \phi_0^2 + \frac{1}{2} m_\sigma^{*2} \sigma^2 \\ & + \frac{1}{2} m_{\sigma^*}^2 \sigma^{*2} + \sum_i \frac{2}{(2\pi)^3} \int_0^{k_{Fi}} d^3k E_i^*, \end{aligned} \quad (2)$$

$$\begin{aligned} p = & \frac{1}{2} m_\omega^{*2} \omega_0^2 + \frac{1}{2} m_\rho^{*2} b_0^2 + \frac{1}{2} m_\phi^2 \phi_0^2 \\ & - \frac{1}{2} m_\sigma^{*2} \sigma^2 - \frac{1}{2} m_{\sigma^*}^2 \sigma^{*2} - \Sigma_0^R \rho \\ & + \frac{1}{3} \sum_i \frac{2}{(2\pi)^3} \int_0^{k_{Fi}} d^3k \frac{k^2}{E_i^*}, \end{aligned} \quad (3)$$

where i runs over the species of baryons and leptons considered in neutron star matter, $E_i^* = \sqrt{k^2 + m_i^{*2}}$ with m_i^* being the Fermion effective mass of species i , and Σ_0^R is the rearrangement term, originating from the density-dependent parameters, to preserve the thermodynamic consistency (Jiang et al. 2007a).

The density dependence of parameters is described by the scaling functions that are the ratios of the in-medium parameters to those in the free space. For the nucleonic sector, we take the scaling functions for the coupling constants of scalar and vector mesons as $\Phi_{\sigma N}(\rho) = (1 - y_i \rho / \rho_0) / (1 + x_i \rho / \rho_0)$ with coefficients x_i and y_i given in (Jiang et al. 2007a,b). For the hyperonic sector, we will give the scaling form for coupling constants below. For hadron masses, the scaling function is given as $\Phi(\rho) = 1 - y\rho/\rho_0$.

For the neutron star matter with hyperonizations, the chemical equilibrium is established on the weak interactions of baryons and leptons. We study chemically equilibrated and charge neutral matter including baryons (N , Λ , Σ , Ξ) and leptons (e , μ). Note that although the baryon chemical potential is modified by the rearrangement term, the chemical equilibrium is independent of this modification.

In the present work, the RMF parameter sets SLC and SLCd (Jiang et al. 2007b) that have no mass scalings for baryons are extended to include the hyperonizations. The main difference between the SLC and SLCd is their prediction for the density dependence of nuclear symmetry energy. More quantitatively, the slope parameter L at saturation density is $L = 92.3$ MeV and 61.5 MeV for the SLC and SLCd, respectively. Assuming all analyses of terrestrial data are equally reliable, a conservative estimate puts L in the range of approximately 25 to 115 MeV and the symmetry energy at normal density $E_{sym}(\rho_0)$ to be between 26 and 34 MeV (Newton et al. 2011; Tsang et al. 2012). However, it is interesting to note that the majority of the analyses of ter-

terrestrial nuclear experiments scatter the L and $E_{sym}(\rho_0)$ values around 60 MeV and 30 MeV, respectively. Several recent analyses of astrophysical observations and phenomena including the mass-radius correlation (Steiner & Gandolfi 2012), the binding energy of neutron stars (Newton & Li 2009), the frequencies of torsional crustal vibrations (Steiner & Watts 2009; Gearheart et al. 2011) and the r -model instability window (Wen et al. 2012), all consistently favor L values less than about 70 MeV. For instance, the latest analysis of neutron star observation puts L in a somewhat lower range of 36 to 55 MeV at 95% confidence level (Steiner & Gandolfi 2012). It is worth noting that the L value from the SLCd model is more consistent with the most stringent constraint on L so far, i.e. approximately $40 < L < 60$ MeV, obtained by combining constraints from analyzing both terrestrial experiments and astrophysical observations (Lattimer & Lim 2012). By comparing calculations with the SLC and SCLd parameter sets we shall examine effects of the symmetry energy on the mass-radius correlation of neutron stars, though the SLCd model can describe the available observations more consistent with conclusions based on other analyses in the literature. The parametrization for hyperons is elaborated in the following. The coupling of mesons with hyperons can generally be given in terms of the parameters $X_{\sigma Y}$, $X_{\omega Y}$, and $X_{\rho Y}$, which are ratios of the meson coupling with hyperons to that with nucleons. Lack of strong constraints on these parameters (Weissenborn et al. 2011a), a variety of choices of these parameters roughly varying from 0.2 to unity were used in practical studies (Glendenning & Moszkowski 1991; Avancini & Menezes 2006). Considering that the nucleonic sector of our models respects chiral limits at high densities, we assume for hyperons two cases: the usual case (UC) that the hyperons have a similar medium effect to nucleons and the separable case (SC) that the meson-hyperon coupling constant is separated into density-dependent and density-independent parts regardless of the chiral limit constraint on the strange sector in hyperons. Nevertheless, the hyperon potentials (Millener et al. 1988; Hausmann & Weise 1989; Fukuda et al. 1998)

$$U_{\Lambda}^{(N)} = -30 \text{ MeV} = -U_{\Sigma}^{(N)}, \quad U_{\Xi}^{(N)} = -18 \text{ MeV}, \quad (4)$$

in nuclear matter at saturation density are used to preserve the relation between the vector and scalar meson coupling constants. Note that the repulsive Σ hyperon potential is invoked here (Mares et al. 1995; Noumi et al. 2002). For the strange mesons, we adopt the density-independent coupling constants in both cases for simplicity. The potentials for the Λ and Ξ hyperons in Ξ matter $U_{\Lambda}^{(\Xi)} = U_{\Sigma}^{(\Xi)} = U_{\Xi}^{(\Xi)} = -40$ MeV are used to obtain the coupling constants of the strange mesons (For the details, see (Jiang 2006; Schaffner & Gal 2000)).

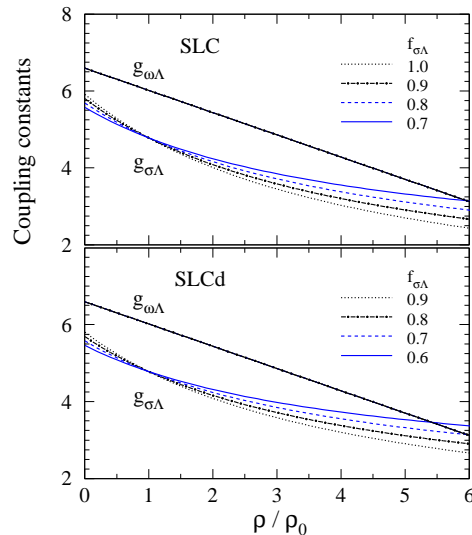


Fig. 1.— (Color online) Coupling constants of the σ and ω mesons with the Λ hyperon as a function of density.

The ratio parameters for coupling constants in the UC are assumed to be density-independent. In the SC, we consider following scaling functions for the meson-hyperon coupling constants that consist of two terms:

$$\begin{aligned} \Phi_{\omega\Lambda}(\rho) &= \Phi_{\omega\Sigma}(\rho) = \frac{1}{3}\Phi_{\omega N}(\rho_0) + \frac{2}{3}\Phi_{\omega N}(\rho), \\ \Phi_{\omega\Xi}(\rho) &= \frac{2}{3}\Phi_{\omega N}(\rho_0) + \frac{1}{3}\Phi_{\omega N}(\rho), \\ \Phi_{\sigma Y}(\rho) &= (1 - f_{\sigma Y})\Phi_{\sigma N}(\rho_0) + f_{\sigma Y}\Phi_{\sigma N}(\rho), \end{aligned} \quad (5)$$

where ρ_0 is the saturation density and $f_{\sigma Y}$ is an

adjustable constant. The scaling functions $\Phi_{\rho\Sigma}$ and $\Phi_{\rho\Xi}$ for the ρ meson are taken the same as those of the ω meson. Note that $\Phi_{\omega N}(\rho_0)$ and $\Phi_{\sigma N}(\rho_0)$ are just constants. The factors before $\Phi(\rho_0)$ and $\Phi(\rho)$ implied from constituent quark compositions play a role in averaging on the hadron level the coupling constant between the density-dependent part originating from the chiral limit and the density-independent part that is presumably attributed to the strange sector in hyperons. The form in (5) produces the relation $\Phi_{iY} \equiv \Phi_{iN}$ at saturation density. Thus, we do not need to readjust the parameter $g_{\sigma Y}(\rho_0)$ as $f_{\sigma Y}$ changes. For a few choices of $f_{\sigma\Lambda}$, we plot the meson- Λ hyperon coupling constants in Fig. 1. It is seen that the larger the $f_{\sigma Y}$, the smaller the $g_{\sigma Y}$ at high densities.

3. Results and discussions

Since the parameters for the nucleonic sector of the SLC and SLCd are clearly given in (Jiang et al. 2007b), we just list in table 1 the parameters for the hyperonic sector. We see in table 1 that in the same case all parameters but $g_{\rho\Xi}^0$ are the same for the models SLC and SLCd. This is because the unique difference between the models SLC and SLCd is that the latter has a softer symmetry energy than the former. Since the neutron star properties are rather insensitive to the coupling parameters of Σ and Ξ hyperons owing to their small fractions in the core of neutron stars, for simplicity we take $f_{\sigma\Sigma} = f_{\sigma\Xi} = f_{\sigma\Lambda}$ for the SC in the calculation. For the similar reason, we prefer the choice $X_{\omega\Lambda} = X_{\omega\Sigma} = X_{\omega\Xi}$ in the UC calculation, unless otherwise denoted. For the ρ meson in the UC, the usual relation $X_{\rho\Sigma} = 2X_{\rho\Xi} = 2$ is used. In both the SC and UC, the $g_{\rho\Lambda}^*$ is zero. Note that all parameters used in this work for hyperons meet the relation (4).

As a well-known consequence, the emergence of the hyperon degree of freedom results in the softening of the EOS. While the models SLC and SLCd that were constructed based on the BR scaling, the softening turns out to be too appreciable at high densities to stabilize the neutron star in the UC with relatively small $X_{\omega\Lambda}$. As shown in the upper panel of Fig. 2, this is related to the rapid decrease of the nucleon effective mass, corresponding to an increasingly large scalar field that pro-

vides the attraction. As known before (Jiang et al. 2007a), the vector coupling constant is decisive to generate a stiff EOS at high densities. Thus, the stiffening of the EOS can follow from increasing the parameter $X_{\omega\Lambda}$. With larger $X_{\omega\Lambda}$, for instance, $X_{\omega\Lambda} = 0.9$, the EOS is stiffened to recover the stability of neutron stars. For the SC, the EOS can be stiffened by increasing the parameter $f_{\sigma Y}$, since the latter results in the decrease of the scalar coupling constant, as shown in Fig. 1. Generally, the EOS obtained with the SC is much stiffer than that with the UC. Meanwhile, the accelerating decrease of the baryon effective mass due to the inclusion of hyperons can be greatly suppressed in the SC, as shown in the lower panel of Fig. 2. In Fig. 2, the Λ and Ξ hyperon effective masses are also displayed. The upward shift of hyperon masses at high densities in the lower panel of Fig. 2 is due to the decrease of the source term (namely, the hyperon density) of the strange mesons, also see below. The hyperon effective mass is much larger than the nucleon one. This would justify the use of the different in-medium interactions for hyperons and nucleons in the SC.

The dropping of the baryon effective mass in chemically equilibrated matter associates tightly with the beginning density and fractions of hyperons. In Fig. 3, we display the particle fractions as a function of density. We see that the fractions of hyperons are rather sensitive to the variation of the in-medium interactions. More noticeably, quite large differences between the left and right panels can be observed. For instance, in the UC (left panel), the interval between the Λ and Ξ^- beginning densities depends sensitively on the ratios of coupling constants, although the relation (4) is always satisfied, while in the SC such a sensitivity does not exist. Moreover, the emergence of the Σ hyperon depends on the model interaction. The Σ hyperon does not appear in the SC. Remarkably, with the increase of density, the hyperon fractions in the SC tend downwards till to disappear after reaching the maximum, as shown in the right panel of Fig. 3. The occurrence of this phenomenon is due to the fact that the vector meson-hyperon coupling constant $g_{\omega Y}^*$ has a weaker density dependence [see Eq.(5)] than the meson-nucleon coupling constant $g_{\omega N}^*$. At high densities, $g_{\omega Y}^*$ exceeds $g_{\omega N}^*$, and so do the vector potentials. The chemical equilibrium thus

Table 1: Meson-hyperon coupling constants in various cases with models SLC and SLCd. In the UC, we tabulate the values with $X_{\omega\Lambda} = X_{\omega\Sigma} = X_{\omega\Xi} = 0.9$. The coupling constants in the medium are obtained as $g_{iY}^* = g_{iY}^0 \Phi_{iY}(\rho)$. In the UC, $g_{iY}^0 = g_{iY}(\rho = 0)$, while in the SC they are not equal. In the SC, the parameters listed here are free of the parameter $f_{\sigma Y}$. For the couplings with the Σ hyperon, we take in the calculation the relations: $g_{\omega\Sigma}^0 = g_{\omega\Lambda}^0$ and $g_{\rho\Sigma}^0 = 2g_{\rho\Xi}^0$.

Model	Case	$g_{\sigma^*\Lambda}$	$g_{\sigma^*\Sigma}$	$g_{\sigma^*\Xi}$	$g_{\sigma\Lambda}^0$	$g_{\sigma\Sigma}^0$	$g_{\sigma\Xi}^0$	$g_{\omega\Lambda}^0$	$g_{\omega\Xi}^0$	$g_{\rho\Xi}^0$
SLC	SC	6.146	7.651	9.764	5.920	3.861	3.063	6.884	3.442	3.802
	UC	6.875	10.117	10.681	7.632	5.573	7.220	9.293	9.293	3.802
SLCd	SC	6.146	7.651	9.764	5.920	3.861	3.063	6.884	3.442	5.776
	UC	6.875	10.117	10.681	7.632	5.573	7.220	9.293	9.293	5.776

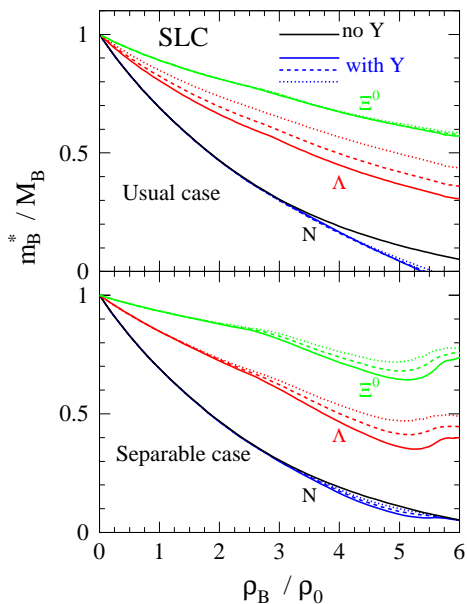


Fig. 2.— (Color online) Baryon effective masses as a function of density in the UC and SC with the SLC. Three curves (solid, dashed and dotted) of the UC in the upper panel are calculated with $X_{\omega\Xi} = 0.6$ and $X_{\omega\Lambda} = 2/3, 0.8$ and 0.9 , respectively. In the lower panel, three curves (solid, dashed and dotted) of the SC are obtained with $f_{\sigma\Lambda} = f_{\sigma\Xi} = 0.7, 0.8$ and 0.9 , respectively.

makes the hyperon Fermi momenta and fractions lower. As an application in studying properties of neutron stars, this actually results in the exclusion of hyperons in the core of neutron stars and accordingly the re-stiffening of the EOS at high densities. In addition to our scheme, we note that there are other attempts to decrease the number of hyperons in neutron stars. For instance, different couplings of a new boson to hyperons and nucleons were proposed to decrease the number of hyperons (Krivoruchenko et al. 2009). Including the nonlinear self-interactions involving a vector meson with hidden strangeness, Bednarek et al. found that the onset density of hyperons can be as high as $3\rho_0$ accompanied by smaller fractions of hyperons (Bednarek et al. 2011). In (Takatsuka et al. 2002; Tsuruta et al. 2009), however, hyperons were found to appear above $4\rho_0$ and thus played a rather limited role in the EOS of neutron star matter. In this work, we find that the onset density of hyperons in the SC can vary upwards within the region $2.2 - 3\rho_0$ as the ratio of vector meson coupling $g_{\omega\Lambda}^0/g_{\omega N}^0$ increases from 0.2 to 0.8 (In table 1, this ratio is $2/3$), while the hyperon fractions get suppressed significantly at larger onset densities. A large rise of this density up to $4.5\rho_0$ can be obtained. However, the binding relation (4) should then be reduced to $U_{\Lambda}^{(N)}(\rho_0) = 0$ MeV. In this case, the hyperon fraction becomes so small that the hyperonic constituents become unimportant. On the quark level, it is interesting to see that the mechanism of small numbers of strange quarks in hybrid stars was explored within a specific quark model (Buballa et al. 2004).

We mention that the baryon fractions in neu-

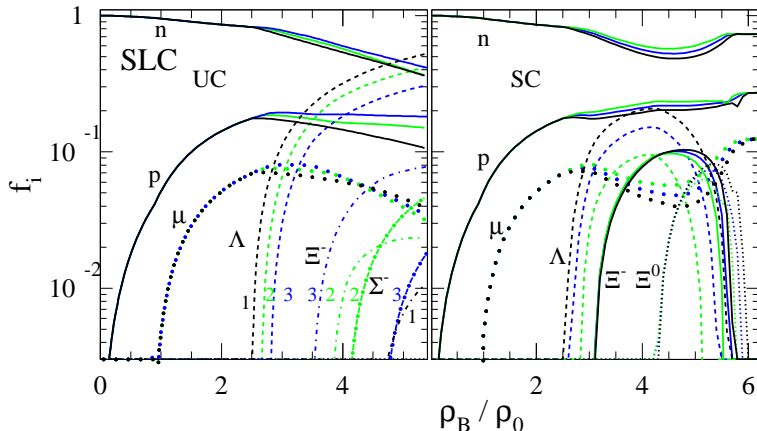


Fig. 3.— (Color online) Particle fractions in the UC and SC with the model SLC as a function of density. In the UC (left panel), three curves for each particle, e.g., denoted by the number 1, 2, and 3, are calculated with $X_{\omega\Lambda} = 2/3, 0.8$ and 0.9 , respectively, while $X_{\omega\Sigma} = 0.9$. The same number in the left panel denotes the results obtained with the same parameters. In the SC (right panel), three curves for each particle, for instance, in a rising order of the Λ hyperon appearance, are obtained with $f_{\sigma\Lambda} = f_{\sigma\Sigma} = 0.7, 0.8$ and 0.9 , respectively.

neutron stars are also sensitive to the symmetry energy. In (Jiang 2006), it was illustrated that the onset density for hyperons increases moderately with the softening of the symmetry energy. For the same reason, the onset density for hyperons with the SLCd is about $0.2\rho_0$ larger than those with the SLC. To save space herein, we do not display particle fractions with the SLCd in a figure similar to Fig. 3.

Although the emergence of hyperons is a cause for softening the nuclear EOS, the specific behavior relies indeed on the in-medium interactions, as clearly shown in Fig. 4. The softening persists at high densities for the UC. However, the softening is succeeded by a stiffening in the SC where hyperons feel a different in-medium interaction from nucleons. Looking back to the right panel of Fig. 3, we see that the stiffening of the EOS occurs with the suppression of hyperon fractions. As the hyperon vanishes, the EOS returns to the normal EOS without hyperons. As shown in Fig. 4, the

EOS evolves to become stiffer than the normal one with increasing density. The neutron star matter thus transits to the normal isospin-asymmetric matter prior to the vanishing of hyperons. This eventually leaves a limited density window allowing the existence of hyperons in neutron stars. Interestingly, we find that the influence of the hyperonization in the SLCd model falls prominently, as compared to the SLC model. This is attributed to the larger onset density of hyperons with the SLCd due to the softening of the symmetry energy, as mentioned above.

In the UC, since the nucleon effective mass vanishes at certain critical density, we need to consider the EOS beyond the critical density. Though the relationship between the chiral restoration and deconfinement occurrence is still discussed, it is nevertheless a convenient and usual way to neglect the distinction between them. Beyond the critical density, we thus adopt a quark matter EOS described by the MIT model with the ap-

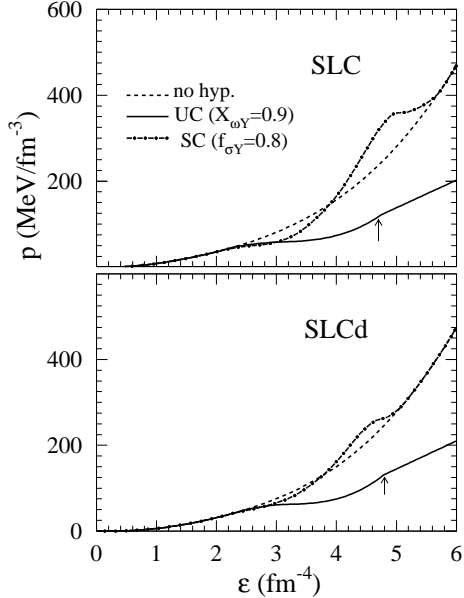


Fig. 4.— EOS of isospin-asymmetric matter with models SLC and SLCd. Curves are obtained with parameters listed in Table 1. The arrow indicates the critical point to quark matter. The result including the muon but without hyperons is also depicted for comparisons.

propriate bag parameter $[(179.5 \text{ MeV})^4]$ to connect smoothly the hadron matter and quark matter EOSs. The connection to the quark matter further softens the EOS, as shown in Fig. 4.

We now turn to the consequences of hyperonizations on properties of neutron stars. In particular, it is interesting to see whether our model with hyperonization can give properties of neutron stars that are compatible with the recent observation of the millisecond pulsar J1614-2230. The mass of this pulsar was accurately determined to be $1.976 \pm 0.04 M_\odot$ (Demorest et al. 2010). It was concluded that such a large mass can rule out almost all currently proposed hyperon equations of state. The mass-radius relation of neutron stars is obtained from solving the standard TOV equation with the nuclear EOS being spec-

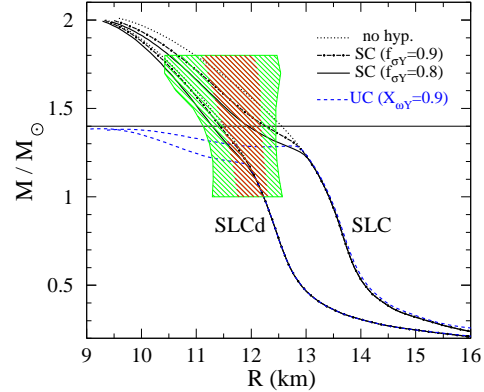


Fig. 5.— (Color online) Mass-radius relation of neutron stars in the UC and SC with the SLC and SLCd. In the SC, two curves are obtained with $f_{\sigma Y} = 0.8$ and 0.9 , respectively. The hatched areas give the probability distributions with 1σ (red) and 2σ (green) confidence limits for $r_{ph} \gg R$ summarized in (Steiner et al. 2010).

ified above. For the low-density crust, we adopt the EOS in (Baym et al. 1971; Iida & Sato 1997). It is seen in Fig. 5 that all EOS's of the SC can produce neutron stars with the maximum mass around $2M_\odot$ and with the corresponding radius ranging from 9.3 to 9.5 km. Since the maximum mass of neutron stars is more sensitive to the EOS at high densities, it is understandable that the EOS including hyperonization at intermediate densities can lead to masses compatible with that of the pulsar J1614-2230. Thus, the EOS with hyperonization can not be simply ruled out. Of course, the hyperon fraction in neutron stars with the SC is rather limited, as compared to that with the UC. In addition, a subtle factor affecting the hyperonization is the density dependence of nuclear symmetry energy. Due to the softening of the symmetry energy in the SLCd, the hyperonization in the SC becomes unimportant for the EOS of neutron star matter, see Fig. 4, which equivalently expels most hyperons in neutron stars. Consequently, the mass-radius relation with the SLCd is almost independent of the parameter $f_{\sigma Y}$ in the

SC, as shown in Fig. 5. For the UC, it looks undoubtedly that the EOS is ruled out by the recent observation (Demorest et al. 2010), since the maximum mass of neutron stars in this case just sprints to $1.4M_{\odot}$ with a much compacter size than the canonical neutron star without hyperons.

It is worth adding here some discussions about the influence of the symmetry energy on the radii of neutron stars. It is now well established that the maximum mass of neutron stars is dominated by the high-density behavior of the EOS, while the radius is primarily determined by the slope of the symmetry energy at intermediate densities ($1 - 3\rho_0$) (Lattimer & Prakash 2001, 2004; Steiner et al. 2005; Xu et al. 2009). The large difference between the radii of low-mass neutron stars obtained with the SLC and SLCd can be attributed to the difference in the slope parameter L . As discussed in detail earlier in ref. (Fattoyev & Piekarewicz 2010), the central density of an 18 - 20 km star is near ρ_0 , and the crust ends approximately at $(1/3 - 1/2)\rho_0$. In this density range, the pressure is dominated by the symmetry energy and not the incompressibility of symmetric nuclear matter. Our results shown in Fig. 5 are consistent with those in ref. (Fattoyev & Piekarewicz 2010). For the $1.4M_{\odot}$ neutron stars in the SC, we see however that the inclusion of hyperons reduces moderately the range of the neutron star radius. For instance, the radius ranges from 11.4km with the SLCd to 12.3km with the SLC for $f_{\sigma Y} = 0.9$, which are well situated in the domain extracted by Steiner et al. (Steiner et al. 2010). With the emergence of hyperons, the sensitivity of the star radius to the symmetry energy is reduced clearly. This is because the Λ -hyperon, being the dominant component of hyperons, is an isospin scalar. The suppression of the isovector potential $g_{\rho}^*b_0$ due to the appearance of Λ hyperons (Jiang 2006) results in the reduction of the pressure of asymmetric matter and thus the star radius, while the magnitude of the suppression depends on the specific values of the symmetry energy and hyperon fraction. As a result, the less sensitivity of the star radius to differences in the symmetry energy is observed in calculations with both the SC and UC. In Fig. 5, we also include the constraints of mass-radius trajectories for $r_{ph} \gg R$ obtained by Steiner et al. in (Steiner et al. 2010). Our results in the SC are

either within (for SLCd) or not very far off (for SLC) the constrained region, though the inclusion of hyperons seems to tilt the vertical trajectories. For low-mass neutron stars, the radii with the SLC are predicted to go beyond the optimal region extracted very recently in (Steiner et al. 2012), unless some other scenarios that allow a loose extension of the radii are invoked to extract the radius constraints (Suleimanov et al. 2011; Zhang et al. 2007). However, the maximum mass of neutron stars is almost independent of the slope L and the radii of low-mass neutron stars. In our cases, the maximum mass is only reduced by about 1% by softening the symmetry energy from the model SLC to SLCd. On the other hand, it is known that the measurements of the neutron star radii are far less precise than the mass measurements, see, e.g., refs. (Suleimanov et al. 2011; Zhang et al. 2007) and references therein. We note that an option of $r_{ph} = R$ can cause a visible slanting of the vertical trajectories (Steiner et al. 2010). The agreement of our results can thus be better with the constraints obtained for $r_{pc} = R$.

We note that there had been a few endeavors in the past to involve the hyperons in heavy neutron stars either by invoking strong repulsions for hyperons or pushing upwards the onset density of hyperons (Hofmann et al. 2001; Takatsuka et al. 2002; Stone et al. 2007; Dexheimer & Schramm 2008; Bednarek et al. 2011; Weissenborn et al. 2011a). The main purpose of our work is to constrain the in-medium hyperon potentials using the 2 solar mass constraint of neutron stars. This indeed requires strong repulsions for hyperons. Due to different density-dependencies of nucleonic and hyperonic potentials in the SC, the hyperonic vector potential exceeds the nucleonic one, leading to a very significant suppression of hyperons at high densities. As a result, the hyperons would exist in a shell of neutron star core even with a small L value.

Besides the effect of hyperonization on the static properties, another consequence of the hyperonization is on the thermal evolution of neutron stars. For the SC in SLC, we see from Fig. 5 that Λ hyperons start to appear above $2.5\rho_0$. At this central density the neutron star mass is about $1.2M_{\odot}$. For most observed neutron stars that have larger masses, it appears that the direct Urca (DU) process with nucleons (Lattimer et al. 1991) and/or

hyperons (Prakash et al. 1992) would occur since the proton fraction in the neutron star matter with hyperonization can be in excess of the DU threshold (14%) with the SC. According to the thermal evolution of observed neutron stars analyzed in (Page et al. 2004; Yakovlev & Pethick 2004), the fast cooling with the DU processes seemed to be excluded in most neutron stars except the massive ones. Slower cooling is possible when the neutrino emissivity can be suppressed by the superfluidity of constituent particles like nucleons and hyperons when the temperature falls below the critical temperature. Page et al. set a stringent requirement for the critical temperature of neutron superfluidity without which enhanced cooling from DU processes may be needed in at least half of the observed young cooling neutron stars (Page et al. 2009). While the DU cooling involving nucleons only was regarded to be too fast, it was pointed out by Tsuruta et al. that the DU cooling with hyperons in neutron stars can be compatible with the observations, provided that the hyperon superfluidity is appropriately accounted for (Tsuruta et al. 2009). In our models with the SC, the hyperonization can thus be favorable to make up the potential incompatibility in the thermal evolution by considering the hyperon superfluidity. On the other hand, the threshold mass of neutron stars which allow the DU process increases with the softening of the symmetry energy due to which the proton fraction exceeds the threshold value at larger densities. For instance, this mass is around $1.3M_{\odot}$ with the SC of the model SLCd, and the threshold density for the DU process is about $4\rho_0$, which is coincidentally the onset density of hyperons in (Tsuruta et al. 2009).

Finally, we discuss some details concerning the in-medium interactions for hyperons. Constrained by the large mass of observed pulsars, it is favorable for us to select the in-medium interactions for hyperons in the SC. It is however interesting to find that the single-particle potentials for hyperons in the UC and SC almost overlap in a large density domain ranging from zero density to intermediate density. The significant departure appears only at high densities (roughly $\geq 4\rho_0$). Especially at lower densities, the SC and UC descriptions give rather limited differences in single-particle properties. This thus indicates that without compromising the suc-

cess in describing properties of hypernuclei, one can constrain significantly the high-density hyperon interactions with the large mass of neutron stars. In addition, we have noticed that many efforts using various quark models with the postulate of strong interactions and/or color superconductivity can also lead to large-mass hybrid stars (Alford et al. 2005; Klähn et al. 2007; Ippolito et al. 2008; Weissenborn et al. 2011b; Bonanno & Sedrakian 2011) with stiff EOS's at high densities. Our models respecting chiral limits possess the similarly stiff EOS at high densities. On the other hand, neutron stars may be composed of more complicated constituents including quarks and meson condensates. It is useful to consider these non-baryonic degrees of freedom and their interplay with hyperons to constrain more quantitatively the in-medium interactions for hyperons. However, this is beyond the scope of the present work.

4. Summary

The density-dependent relativistic mean-field model, which was constructed to respect the chiral symmetry restoration at high densities in terms of in-medium hadron properties according to the Brown-Rho scaling, is extended to include the hyperonization in isospin-asymmetric matter. We examined effects of the in-medium hyperon interactions on properties of neutron stars. It is found that the maximum mass of neutron stars can constrain significantly the in-medium hyperon interactions. In particular, assuming two categories of in-medium interactions for hyperons, we investigated their distinct roles in hyperonizations and properties of neutron stars. With different in-medium interactions for hyperons and nucleons (i.e., the SC case), a maximum neutron star mass of $2M_{\odot}$ can be obtained with the model where the nucleonic EOS is consistent with the terrestrial nuclear laboratory data. The result in the SC is compatible with recent observation on the mass of the millisecond pulsar J1614-2230. In this scheme, the number of hyperons is limited in neutron stars. Interestingly, we also found that the softening of the symmetry energy can play an important role in further reducing hyperons in neutron stars. On the contrary, the scheme that adopts similar in-medium interactions for both hyperons and nucleons (i.e., the UC case) can give a maximum

neutron star mass of only about $1.4M_{\odot}$. Nevertheless, the hyperonization in both cases reduces clearly the sensitivity of the neutron star radius to the difference in the nuclear symmetry energy.

Acknowledgement

We would like to thank William Newton for his very helpful and constructive comments. One of the authors (J.W.Z.) would like to thank Ang Li and Zhao-Qing Feng for useful discussions and expresses his sincere gratitude to Dr. Song Dan at the affiliated Hospital of Nanjing Medical University for his great help during the time of this work. This work was supported in part by the National Natural Science Foundation of China under Grant Nos. 10975033, 10975097 and 11135011, the China Jiangsu Provincial Natural Science Foundation under Grant No.BK2009261, the China Major State Basic Research Development Program under Contract No. 2007CB815004, Shanghai Rising-Star Program under Grant No.11QH1401100, the “Shu Guang” project supported by Shanghai Municipal Education Commission and Shanghai Education Development Foundation, the Program for Professor of Special Appointment (Eastern Scholar) at Shanghai Institutions of Higher Learning, the Science and Technology Commission of Shanghai Municipality (11DZ2260700), the US NSF under grants PHY-0757839 and PHY-1068022 and NASA under grant NNX11AC41G issued through the Science Mission Directorate.

REFERENCES

Alford, M., Braby, M., Paris, M., & Reddy, S., 2005, *ApJ*, 629, 969

Avancini, S. S., & Menezes, D. P., 2006, *Phys. Rev. C*, 74, 015201

Baym, G., Pethick, C., & Sutherland, P., 1971, *ApJ*, 170, 299

Bednarek, I., Haensel, P., Zdunik, J., Bejger, M., & Manka, R., 2011, arXiv:1111.6942 [astro-ph.SR]

Bonanno, L., & Sedrakian, A., 2012, *Astron. & Astrophys.*, 539, A16

Brown, G. E., & Rho, M., 1991, *Phys. Rev. Lett.*, 66, 2720 (1991).

Brown, G. E., & Rho, M., 2005, *nucl-th/0509001*; *ibid. nucl-th/0509002*

Brown, G. E., Holt, J. W., Lee, C.-H., & Rho, M., 2007, *Phys. Rep.*, 439, 161

Buballa, M., Neumann, F., Oertel, M., & Shovkovy, I., 2004, *Phys. Lett. B*, 595, 36

Chen, L. W., Ko, C. M., & Li, B. A., 2005, *Phys. Rev. Lett.*, 94, 032701

Danielewicz, P., Lacey, R., & Lynch, W. G., 2002, *Science*, 298, 1592

Demorest, P. B., Pennucci, T., Ransom, S. M., Roberts, M. S. E., & Hessels, J. W. T., 2010, *Nature*, 467, 1081

Dexheimer, V., & Schramm, C., 2008, *ApJ*, 683, 943

Fattoyev, F. J., & Piekarewicz, J., 2010, *Phys. Rev. C*, 82, 055803

Friedman, E., & Gal, A., 2007, *Phys. Rep.*, 452, 89

Fukuda, T., et al., (E224 Collaboration), 1998, *Phys. Rev. C*, 58, 1306

Gearheart, M., Newton, W. G., Hooker, J., & Li, B. A., 2011, *MNRAS*, 418, 2343

Glendenning, N. K., 1985, *ApJ*, 293, 470

Glendenning, N. K., & Moszkowski, S. A., 1991, *Phys. Rev. Lett.*, 67, 2424

Glendenning, N. K., 2000, *Compact Stars* (Berlin: Springer)

Glendenning, N. K., 2001, *Phys. Rep.*, 342, 393

Hausmann, R., & Weise, W., 1989, *Nucl. Phys. A*, 491, 601

Hofmann, F., Keil, C., & Lenske, H., 2001, *Phys. Rev. C*, 64, 025804

Iida, K., & Sato, K., 1997, *ApJ*, 477, 294

Ippolito, N. D., Ruggieri, M., Rischke, D. H., Sedrakian, A., & Weber, F. 2008, *Phys. Rev. D*, 77, 023004

Jiang, W. Z., 2006, *Phys. Lett. B*, 642, 28

- Jiang, W. Z., Li, B. A., & Chen, L. W., 2007a, *Phys. Lett. B*, 653, 184
- Jiang, W. Z., Li, B. A., & Chen, L. W., 2007b, *Phys. Rev. C*, 76, 054314
- Klähn, T., Blaschke, D., Sandin, F., et al., 2007, *Phys. Lett. B*, 654, 170
- Krivoruchenko, M. I., Simkovic, F., & Faessler, A., 2009, *Phys. Rev. D*, 79, 125023
- Lattimer, J. M., Prakash, M., Pethick, C. J. & Haensel, P., 1991, *Phys. Rev. Lett.*, 66, 2701
- Lattimer, J. M., & Prakash, M., 2001, *ApJ*, 550, 426
- Lattimer, J. M., & Prakash, M., 2004, *Science*, 304, 536
- Lattimer, J. M., & Lim, Y., 2012, *ArXiv:1203.4286v1*
- Li, B. A., & Chen, L. W., 2005, *Phys. Rev. C*, 72, 064611
- Li, B. A., Chen, L. W., & Ko, C. M., 2008, *Phys. Rep.*, 464, 113
- Li, H., Luo, X. L., Jiang, Y., & Zong, H. S., 2011, *Phys. Rev. D*, 83, 025012
- Mares, J., Friedman, E., Gal, A., & Jennings, B. K., 1995, *Nucl. Phys. A*, 594, 311
- Millener, D. J., Dover, C. B., & Gal, A., 1988, *Phys. Rev. C*, 38, 2700
- Nice, D. J., Splaver, E. M., Stairs, I. H., Loehmer, O., et al., 2005, *ApJ*, 634, 1242
- Nice, D. J., Stairs, I. H., & Kasian, L. E., 2008, in *AIP Conf. Ser.* 983, 40 *Years of Pulsars: Millisecond Pulsars, Magnetars and More*, ed. C. Bassa, Z. Wang, A. Cumming, and V. M. Kaspi (AIP: New York), 453
- Newton, W., & Li, B. A., 2009, *Phys. Rev. C*, 80, 065809
- Newton, W., Gearheart, M., & Li, B. A., 2011, *arXiv:1110.4043*.
- Noumi, H., et al., 2002, *Phys. Rev. Lett.*, 89, 072301
- Özel, F., 2006, *Nature*, 441, 1115
- Page, D., Lattimer, J. M., & Prakash, M., & Steiner, A. W., 2004, *ApJS*, 155, 623
- Page, D., Lattimer, J. M., & Prakash, M., & Steiner, A. W., 2009, *ApJ*, 707, 1131
- Pagliara, G., & Schaffner-Bielich, J., 2008, *Phys. Rev. D*, 77, 063004
- Piekarewicz, J., 2007, *Phys. Rev. C*, 76, 064310
- Prakash, M., Prakash, M., Lattimer, J. M., & Pethick, C. J., 1992, *ApJ*, 390, L77
- Prakash, M., Bombaci, I., Prakash, M., J. Ellis, P., J., Lattimer, J. M., & Knorren, R., 1997, *Phys. Rep.*, 280, 1
- Schaffner-Bielich, J., & Gal, A., 2000, *Phys. Rev. C*, 62, 034311
- Schulze, H. J., & Rijken, T., 2011, *Phys. Rev. C*, 84, 035801
- Song, C., 2001, *Phys. Rep.*, 347, 289
- Steiner, A. W., Prakash, M., Lattimer, J. M., & Ellis, P. J., 2005, *Phys. Rep.*, 411, 325
- Steiner, A. W., & Watts, A. L., 2009, *Phys. Rev. Lett.*, 103, 181101
- Steiner, A. W., Lattimer, J. M., & Brown, E. F., 2010, *ApJ*, 722, 33
- Steiner, A. W., & Gandolfi, S., 2012, *Phys. Rev. Lett.*, 108, 081102
- Steiner, A. W., Lattimer, J. M., & Brown, E. F., 2012, *arXiv:1205.6871*
- Suleimanov, V., Poutanen, J., Revnivtsev, M., & Werner, K., 2011, *ApJ*, 742, 122
- Stone, J. R., Guichon, P. A., Matevosyan, H. H., & Thomas, A. W., 2007, *Nucl. Phys. A* 792, 341
- Takatsuka, T., Nishizaki, S., Yamamoto, Y., & Tamagaki, R., 2002, *Prog. Theor. Phys. Suppl.*, 146, 279
- Tsang, M. B., et al., 2004, *Phys. Rev. Lett.*, 92, 062701

- Tsang, M. B., et al., 2012, arXiv:1204.0466
- Tsuruta, S., Sadino, J., Kobelski, A., Teter, M. A., Liebmann, A. C., Takatsuka, T., Nomoto, K., & Umeda, H., 2009, ApJ, 691, 621
- Weissenborn, S., Chatterjee, D., & Schaffner-Bielich, J., 2011, arXiv:1112.0234v1 [astro-ph.HE]
- Weissenborn, S., Sagert, I., Pagliara, G., Hempel, M., & Schaffner-Bielich, J., 2011, ApJ, 740, L14
- Wen, D. H., Newton, W. G., & Li, B. A., 2012, Phys. Rev. C, 85, 025801
- Xu, J., Chen, L. W., Li, B. A., & Ma, H. R., 2009, ApJ, 697, 1549
- Xu, R. X., 2003, ApJ, 596, L59
- Yakovlev, D. G., & Pethick, C. J., 2004, ARA&A, 42, 169
- Yasutake, N., Burgio, G. F., & Schulze, H. J., 2011, Phys. Atom. Nucl. 74, 1534, arXiv:1012.1773
- Youngblood, D. H., Clark, H. L., & Lui, Y. W., 1999, Phys. Rev. Lett., 82, 691
- Zhang, C. M., Yin, H. X., Kojima, Y., et al., 2007, MNRAS, 374, 232